Critical scaling of the ac conductivity for a superconductor above T_c

Robert A. Wickham* and Alan T. Dorsey†
Department of Physics, University of Florida, P.O. Box 118 440, Gainesville, Florida 32611-8440
(Received 7 June 1999)

We consider the effects of critical superconducting fluctuations on the scaling of the linear ac conductivity, $\sigma(\omega)$, of a bulk superconductor slightly above T_c in zero applied magnetic field. The dynamic renormalization-group method is applied to the relaxational time-dependent Ginzburg-Landau model of superconductivity, with $\sigma(\omega)$ calculated via the Kubo formula to $O(\epsilon^2)$ in the $\epsilon=4-d$ expansion. The critical dynamics are governed by the relaxational XY-model renormalization-group fixed point. The scaling hypothesis $\sigma(\omega) \sim \xi^{2-d+z} S(\omega\xi^z)$ proposed by Fisher, Fisher, and Huse is explicitly verified, with the dynamic exponent $z \approx 2.015$, the value expected for the $d=3$ relaxational XY model. The universal scaling function $S(y)$ is computed and shown to deviate only slightly from its Gaussian form, calculated earlier. The present theory is compared with experimental measurements of the ac conductivity of $YBa_2Cu_3O_{7-\delta}$ near T_c, and the implications of this theory for such experiments is discussed.

I. INTRODUCTION

The discovery of high-temperature superconductors has, for the first time, made it possible to experimentally probe the critical region of the zero-field normal-superconducting transition since fluctuation effects in these materials are enhanced by the short coherence length and the high-transition temperature T_c. It is natural then to ask: If scaling and universality exist in the critical region, to which universality class does the transition belong? From observations of the effects of critical superconducting fluctuations on thermodynamic properties, such as the penetration depth,[1,2] magnetic susceptibility,[3–5] specific heat[3,6] and thermal expansivity,[7] a consensus is emerging that the zero-field normal-superconducting transition is in the *static* universality class of the three-dimensional, complex order-parameter (3D XY) model. In contrast, the effect of critical fluctuations on transport properties, such as the conductivity, depends on the nature of the *dynamics* near T_c and is much less explored.

In general, conductivity measurements on high-T_c superconductors show an enhanced response above T_c due to the presence of superconducting fluctuations. Outside the critical region this enhancement can be explained in terms of the Aslamazov-Larkin[8] theory of noninteracting, Gaussian fluctuations, and its extensions.[9,10] In these theories the dynamic exponent z associated with the growth of the characteristic order-parameter time scale near T_c appears in the conductivity and takes the value $z=2$. By examining the deviation of z from 2 inside the critical region through linear dc,[3,4,11–14] nonlinear dc,[15–17] and linear ac[18] conductivity measurements, the dynamic universality class can, in principle, be determined. Currently, however, there is much variation in the measured values for z and the dynamic universality class of the zero-field normal-superconducting transition remains uncertain. Unlike dc measurements, measurements of the ac conductivity[18] can test the scaling of the conductivity, $\sigma(\omega)$, over a wide range of frequencies, ω, thereby providing a stringent test of theory. In the experiments of Ref. 18 the ac conductivity exhibits a scaling collapse, which deviates slightly from the Gaussian theory. However, the Gaussian theory is known to break down in the critical region. Thus, to sharpen the comparison between experiment and theory, we go beyond the Gaussian description of fluctuations in this paper and calculate the scaling behavior of the ac conductivity in the critical region of strong, interacting fluctuations.

Fisher, Fisher, and Huse (FFH) (Ref. 19) have argued that near a second-order phase transition, if dynamic scaling holds, the ac fluctuation conductivity should scale as

$$\sigma(\omega) \sim \xi^{2-d+z} S(\omega\xi^z), \tag{1.1}$$

where the correlation length for fluctuations in the superconducting order parameter at temperature T is $\xi \sim |T-T_c|^{-\nu}$ with the static exponent ν, d is the spatial dimensionality, z is the dynamic exponent and $S(y)=S'(y)+iS''(y)$ is a universal, complex function of the scaled frequency $y \sim \omega\xi^z$, with real and imaginary parts S' and S'', respectively. Outside the critical region, and in the dc limit, Eq. (1.1) reduces to the Aslamazov-Larkin theory. Since the conductivity is causal, and also finite for nonzero frequencies, Eq. (1.1) leads to the power-law behavior at T_c

$$\sigma(\omega) \sim (-i\omega)^{-(2-d+z)/z}, \tag{1.2}$$

reflecting the absence of a characteristic time scale at criticality. At T_c the phase

$$\phi(\omega) \equiv \tan^{-1}\left(\frac{S''(\omega\xi^z)}{S'(\omega\xi^z)}\right) \tag{1.3}$$

of the conductivity is independent of frequency, with the value[10]

$$\phi = \frac{\pi}{2}\left(\frac{2-d+z}{z}\right). \tag{1.4}$$

Equations (1.2) and (1.4) allow one to determine the dynamic exponent z independently of the static exponent ν through a measurement of the ac conductivity at criticality. To go beyond these two results and calculate the entire universal scaling function $S(y)$ requires knowledge of the

renormalization-group fixed point that determines the universality class for the dynamics near T_c.

The time-dependent Ginzburg-Landau (TDGL) model of superconductivity provides an appropriate framework in which to study dynamic critical behavior in this system.[20,21] Since this is the first detailed study of the dynamics in the critical region of the superconductor, and given the uncertainty as to which dynamic universality class describes the transition, we consider here only the simplest, relaxational, dynamics for fluctuations in the superconducting order-parameter—model A in the Hohenberg and Halperin classification.[21,22] Previous studies of this model have implemented the Gaussian approximation, where quartic interactions among fluctuations in the Ginzburg-Landau free energy are neglected.[9,10] In this approximation, the conductivity scales as Eq. (1.1) with $\nu=1/2$ and $z=2$, the exponents for the Gaussian fixed point, and the scaling function $S(\omega\xi^2)$ has been explicitly calculated.

In the critical region the Gaussian approximation breaks down since the quartic interactions become important, producing the critical fixed point for the relaxational XY model.[23,24] In the $\epsilon=4-d$ expansion, the exponents for this fixed point are well known.[20] An extrapolation of the $O(\epsilon^2)$ results to three dimensions gives a correlation-length exponent of $\nu\approx 2/3$ and a correlation function exponent of $\eta \approx 0.02$. For relaxational dynamics the dynamic exponent z is, to $O(\epsilon^2)$:[24]

$$z=2+c\,\eta \tag{1.5}$$

with

$$c=6\ln 4/3-1, \tag{1.6}$$

giving $z\approx 2.015$ in three dimensions.

In the critical region, and near four dimensions, we verify that the ac fluctuation conductivity satisfies the FFH scaling hypothesis (1.1) for the relaxational XY-model fixed point. We compute the universal complex scaling form $S(y)$ appearing in Eq. (1.1) to $O(\epsilon^2)$, with the result

$$S(y)=\frac{2z^2}{(d-2+z)(d-2)}\,\frac{1}{y^2}\left[1-\frac{d-2+z}{z}\,iy - (1-iy)^{(d-2+z)/z}\right], \tag{1.7}$$

where $y\sim\omega\xi^z$ and z is given by Eq. (1.5) with Eq. (1.6). In Eq. (1.7), $S(y)$ is normalized so that $S(0)=1$. Equation (1.7) is the main result of this paper, and is the product of a much more involved analysis than that used to determine the exponent z. Sections II–VI provide the details of the calculation. The result (1.7) has the scaling behavior stated in Eq. (1.2). The scaling function $S(y)$ for the critical theory is very close to the Gaussian result calculated earlier (see Fig. 1) since the Gaussian result is given by Eq. (1.7) with $z=2$ and, to $O(\epsilon^2)$,z for the critical theory in three dimensions is only slightly different from two. In Sec. VII we compare the experimental ac conductivity data of Booth *et al.*[18] to the critical theory, extrapolated to three dimensions, and comment in Sec. VIII on the implications of this work for such measurements.

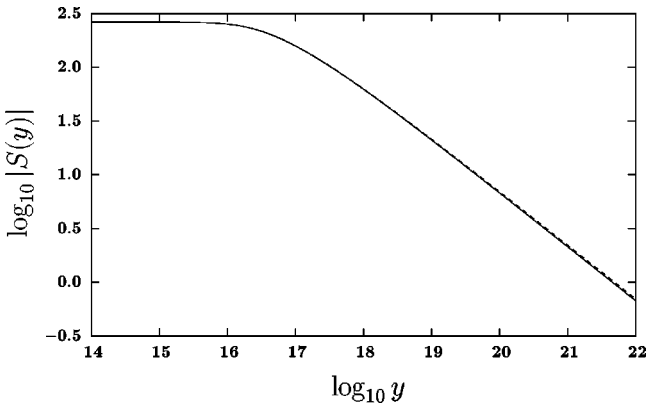

FIG. 1. Comparison of the ac conductivity scaling function $S(y)$, Eq. (1.7), for the relaxational 3D XY critical theory (solid curve) with the scaling function, Eq. (3.7), for the Gaussian theory (dashed curve). To facilitate later comparison with experiments (Ref. 18), the magnitude of $S(y)$ is plotted against the scaled frequency y on a log-log scale.

II. FORMALISM

A. The time-dependent Ginzburg-Landau model of superconductivity

We describe the critical dynamics of a superconductor with a complex order parameter ψ using the relaxational time-dependent Ginzburg-Landau model

$$\frac{\partial\psi}{\partial t}=-\Gamma_0\frac{\delta F}{\delta\psi^*}+\zeta, \tag{2.1}$$

with the Ginzburg-Landau free-energy

$$F=\int d^dr\left(|\nabla\psi|^2+r_0|\psi|^2+\frac{u_0}{2}|\psi|^4\right). \tag{2.2}$$

In Eq. (2.1) Γ_0 is the bare order-parameter relaxation rate. Both Γ_0 and the bare coefficient u_0, which appears in the free energy (2.2), can be considered temperature independent near the transition; however $r_0\sim T-T_{c0}$ changes sign at the mean-field transition temperature T_{c0}, becoming negative for temperatures below T_{c0}. We choose units so that $\hbar=k_BT_c=1$ and $m=1/2$, where m is the mass of a Cooper pair. The superconductor is assumed to be isotropic. The complex noise field ζ in Eq. (2.1) is taken to have zero mean and correlations described by

$$\langle\zeta(\mathbf{r},t)\zeta^*(\mathbf{r}',t')\rangle=2\Gamma_0\delta(\mathbf{r}-\mathbf{r}')\,\delta(t-t'), \tag{2.3}$$

where the brackets $\langle\cdots\rangle$ denote an average over the noise distribution, assumed to be Gaussian. The factor $2\Gamma_0$ in Eq. (2.3) follows from the fluctuation-dissipation theorem and ensures that the system relaxes to the proper equilibrium distribution.

We will work in the symmetric phase, $T>T_c$, with zero applied magnetic field and consider order-parameter fluctuations about a mean of zero. Fluctuations of the vector potential are neglected.[25] Since we will use the Kubo formula to calculate the linear conductivity from the system in zero electric field, an electric field is not included in Eqs. (2.1)–(2.2). In the classification scheme of Hohenberg and Halperin,[21] Eqs. (2.1)–(2.3) constitute model A dynamics for

a two-component (complex) order parameter. Thus our model is in the dynamic universality class of the relaxational XY model.[23,24]

Since the Ginzburg-Landau theory is coarse grained, it contains an ultraviolet (UV) cutoff, Λ (corresponding, for example, to the lattice constant).[26] This cutoff is manifest in the definition of the Fourier transform of the order-parameter,

$$\psi(\mathbf{r},t)=\int_{k\omega}^{\Lambda}\psi(\mathbf{k},\omega)e^{i\mathbf{k}\cdot\mathbf{r}-i\omega t}. \tag{2.4}$$

For convenience, we employ the short forms

$$\int_{k}^{\Lambda}=\int^{\Lambda}\frac{d^dk}{(2\pi)^d} \tag{2.5}$$

$$\int_{\omega}=\int\frac{d\omega}{(2\pi)} \tag{2.6}$$

for the wave-vector and frequency integrals, with the wave-vector integral restricted to $|\mathbf{k}|<\Lambda$. The existence of the cutoff will be crucial when we interpret the results of the theory.

The order-parameter correlation function and the response function are central in what follows. The order-parameter correlation function, $C(\mathbf{k},\omega)$, is defined as

$$C(\mathbf{k},\omega)\equiv\langle\psi(\mathbf{k},\omega)\psi^*(\mathbf{k},\omega)\rangle. \tag{2.7}$$

By adding a source term,

$$F_h=-\int d^dr(h^*\psi+h\psi^*), \tag{2.8}$$

to the free energy (2.2) we can define the (linear) response function, $G(\mathbf{k},\omega)$, as

$$G(\mathbf{k},\omega)\equiv\left.\frac{\delta\langle\psi(\mathbf{k},\omega)\rangle}{\delta h(\mathbf{k},\omega)}\right|_{h=0}. \tag{2.9}$$

This measures the response of the order parameter to the source h. Near equilibrium, the correlation and response functions are related though the fluctuation-dissipation relation,[27]

$$C(\mathbf{k},\omega)=\frac{2}{\omega}\mathrm{Im}\,G(\mathbf{k},\omega). \tag{2.10}$$

B. The Kubo formula for the conductivity

The linear ac conductivity, $\sigma(\omega)$, for an isotropic material can be defined in terms of the current response, $\mathbf{J}$ (which includes normal and supercurrent contributions), to an infinitesimal applied electric field, $\mathbf{E}$, through

$$\mathbf{J}(\omega)=\sigma(\omega)\mathbf{E}(\omega). \tag{2.11}$$

Since the quantities in Eq. (2.11) are evaluated at zero wave-vector we suppress their wave-vector dependence. The conductivity is complex and has a real dissipative response, σ', and an imaginary reactive response, σ'':

$$\sigma(\omega)=\sigma'(\omega)+i\sigma''(\omega). \tag{2.12}$$

In linear response, the conductivity is related to a current correlation function *via* the Kubo formula.[28] Near T_c strong superconducting fluctuations give a singular contribution to the conductivity which dominates the nonsingular contribution due to normal electrons. Thus we may use the Kubo formula to calculate the real part of the conductivity due to superconducting fluctuations from the supercurrent correlation function, evaluated at $\mathbf{E}=0$:[9]

$$\sigma'(\omega)=\frac{1}{2d}\langle\mathbf{J}_s(\omega)\cdot\mathbf{J}_s(-\omega)\rangle|_{\mathbf{E}=0}. \tag{2.13}$$

The supercurrent, $\mathbf{J}_s$ is

$$\mathbf{J}_s(\mathbf{r},t)=-ie_0(\psi^*\nabla\psi-\psi\nabla\psi^*), \tag{2.14}$$

where e_0 is the bare charge of a Cooper pair. The imaginary part of the conductivity can be obtained by applying the Kramers-Kronig relations[28] to Eq. (2.13).

The average in Eq. (2.13) is a four-point order-parameter average since $\mathbf{J}_s$ (2.14) is quadratic in ψ. Quite generally, this four-point average can be written as the sum of a ''disconnected'' product, $\sigma^{(2)}$, of two two-point averages, and a ''connected'' four point-average $\sigma^{(4)}$:

$$\sigma'(\omega)=\sigma^{(2)}(\omega)+\sigma^{(4)}(\omega), \tag{2.15}$$

with

$$\sigma^{(2)}(\omega)=\frac{2e_0^2}{d}\int_{k_1\omega_1}^{\Lambda}k_1^2C(\mathbf{k}_1,\omega_1)C(\mathbf{k}_1,\omega_1+\omega), \tag{2.16}$$

and

$$\sigma^{(4)}(\omega)=\frac{2e_0^2}{d}\int_{k_1\omega_1k_2\omega_2}^{\Lambda}\mathbf{k}_1\cdot\mathbf{k}_2C_c^{(4)}(\mathbf{k}_1,\omega_1,\mathbf{k}_2,\omega_2;\omega), \tag{2.17}$$

where the exact two-point order-parameter correlation function, $C(\mathbf{k},\omega)$, is defined in Eq. (2.7) and

$$\begin{aligned}C_c^{(4)}(\mathbf{k}_1,\omega_1,\mathbf{k}_2,\omega_2;\omega)\equiv\langle&\psi(\mathbf{k}_1,\omega_1)\\&\times\psi^*(\mathbf{k}_1,\omega_1-\omega)\psi(\mathbf{k}_2,\omega_2)\\&\times\psi^*(\mathbf{k}_2,\omega_2+\omega)\rangle_c\end{aligned} \tag{2.18}$$

is the connected four-point order-parameter correlation function.

C. Iterative dynamic perturbation theory

The order-parameter averages (2.7) and (2.18) that appear in Eqs. (2.16) and (2.17) can be expanded as a perturbation series in the bare nonlinear coupling u_0 appearing in Eq. (2.2). Dynamic perturbation theory for the time-dependent Ginzburg-Landau equation, Eq. (2.1), can be implemented either by using a Martin-Siggia-Rose field-theoretical formalism,[29,30] or by a direct iteration of the equation of motion.[20,31] The iterative approach involves less formal machinery and will be used here.

The equation of motion (2.1) can be explicitly written in Fourier space as

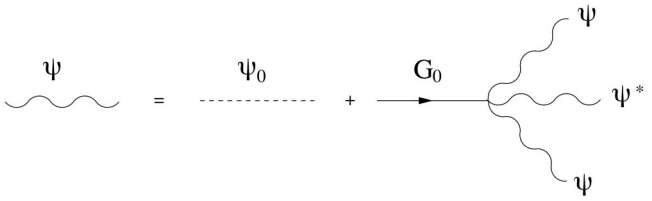

FIG. 2. The diagrammatic representation of the equation of motion (2.19). Wiggly lines correspond to the order parameter ψ (a starred wiggly line is ψ^*). The dotted line represents the Gaussian field ψ_0. The Gaussian response function G_0 (2.21) is shown as a line with an arrow. The vertex, where the response function meets three wiggly lines contains a factor $-u_0$, as well as V (2.22), which conserves wave vector and frequency at the vertex. Iteration corresponds to replacing the wiggly lines on the right-hand side with either the first or second term on the right-hand side. In this way, one generates a series in u_0.

$$\psi(\mathbf{k},\omega)=\psi_0(\mathbf{k},\omega)-u_0G_0(\mathbf{k},\omega)\int_{k_1\omega_1k_2\omega_2k_3\omega_3}^{\Lambda}V\psi(\mathbf{k}_1,\omega_1)\times\psi^*(\mathbf{k}_2,\omega_2)\psi(\mathbf{k}_3,\omega_3), \tag{2.19}$$

where

$$\psi_0(\mathbf{k},\omega)=\frac{1}{\Gamma_0}G_0(\mathbf{k},\omega)\zeta(\mathbf{k},\omega), \tag{2.20}$$

$$G_0(\mathbf{k},\omega)=\left(-\frac{i\omega}{\Gamma_0}+r_0+k^2\right)^{-1}, \tag{2.21}$$

and

$$V=(2\pi)^{d+1}\delta(\mathbf{k}-\mathbf{k}_1+\mathbf{k}_2-\mathbf{k}_3)\delta(\omega-\omega_1+\omega_2-\omega_3). \tag{2.22}$$

The Gaussian theory neglects the nonlinear interaction ($u_0=0$). In this case Eq. (2.19) reduces to $\psi=\psi_0$, and the order parameter is a Gaussian field by virtue of Eq. (2.20) and the fact that ζ is Gaussian. The order-parameter correlation function (2.7) can then be evaluated using Eq. (2.3) and is

$$C_0(\mathbf{k},\omega)\equiv\langle\psi_0(\mathbf{k},\omega)\psi_0^*(\mathbf{k},\omega)\rangle=\frac{2\Gamma_0}{\omega^2+\Gamma_0^2(r_0+k^2)^2}. \tag{2.23}$$

If a term coming from F_h (2.8) is included in the equation of motion (2.19), it is straightforward to show that G_0 (2.21) is the Gaussian response function. A glance at Eqs. (2.21) and (2.23) shows that the Gaussian theory satisfies the fluctuation-dissipation relation, Eq. (2.10).

Since ψ appears in the integral on the right-hand side of Eq. (2.19), this equation can be iterated to produce an expansion for ψ in powers of the bare coupling constant u_0. Averages containing ψ are then expressed as sums of higher-point Gaussian averages over ψ_0, which break up into products of C_0's. To keep track of the algebra, it is helpful to use the graphical representation of Eq. (2.19) shown in Fig. 2. In the graphical context iteration corresponds to ''putting branches on the tree'' and averaging corresponds to joining two conjugate dashed lines (ψ_0) to form a correlation function C_0. By examining all possibilities for joining for a given average, a series of graphs is generated with the proper symmetry factors. In dynamical perturbation theory there are two propagators: the response function G_0, denoted by an arrow, and the correlation function C_0, denoted by a line with a circle on it. Wave vector and frequency are assigned to these lines on the basis of conservation of wave vector and frequency at the graph vertices, given by V in Eq. (2.22). Wave vectors and frequencies flowing around loops are integrated over. More details of the graph rules can be found in Refs. 20 and 31. An example of this procedure is the self-energy diagram, Fig. 3, and the corresponding algebraic expression (4.5).

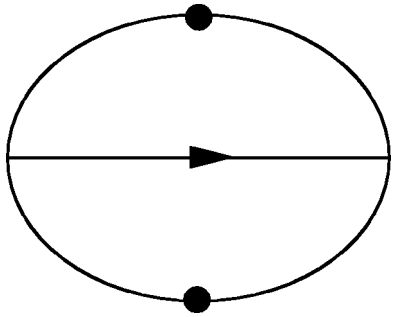

FIG. 3. The Saturn diagram, Σ_s, for the self-energy consists of two loops formed by two correlation functions C_0 (lines with circles) and one response function G_0 (line with an arrow). Wave vector and frequency flow through the diagram in accordance with the discussion in Sec. II C.

D. Renormalization of the theory and the *XY* fixed point

It is well known that, near criticality, the expansion of the theory in terms of the bare ''coupling constant'' u_0 produces infrared (IR) divergences due to the diverging correlation length. One method to treat these divergences and produce sensible results is to reorganize the expansion as an expansion in $\epsilon=4-d$. To accomplish this, we must first ensure that all UV divergences (we take $\Lambda\to\infty$) as $\epsilon\to0$ are absorbed into a renormalization of the bare quantities r_0, u_0, e_0, and Γ_0. It is computationally convenient to dimensionally regularize the theory and renormalize *via* minimal subtraction.[30,32] Following renormalization, we must relate u_0 (or, more precisely the suitably renormalized and dimensionless coupling $\bar{u}$, defined below) to ϵ by examining the fixed-point structure of the renormalization-group (RG) flow. Below, we examine the renormalization of the theory and the RG fixed point in more detail.

We define the renormalized coupling constant, u, in terms of the bare coupling constant, u_0, by

$$u\equiv Z_uu_0, \tag{2.24}$$

and define the dimensionless, renormalized coupling constant, $\bar{u}$ as

$$\bar{u}\equiv\frac{S_d}{2(2\pi)^d}u\kappa^{-\epsilon}, \tag{2.25}$$

where κ is an arbitrary wave-vector scale and $S_d=2\pi^{d/2}/\Gamma(d/2)$ is the surface area of the unit sphere in d dimensions. The renormalization constant $Z_u=1+O(\bar{u})$.[32]

Since only $\overline{u^2}$ will appear in the conductivity, and we neglect terms of $O(\overline{u^3})$ and higher, we may approximate $Z_u = 1$.

Renormalization of the bare response function (2.9) provides the remaining renormalization constants. The bare inverse response function including self-energy corrections, Σ, may be written

$$G^{-1}(\mathbf{k},\omega) = G_0^{-1}(\mathbf{k},\omega) - \Sigma(\mathbf{k},\omega). \tag{2.26}$$

The renormalized inverse response function $G_R^{-1}(\mathbf{k},\omega)$ may be expressed in terms of the bare quantity (2.26) by

$$G_R^{-1}(\mathbf{k},\omega) \equiv Z_\psi G^{-1}(\mathbf{k},\omega), \tag{2.27}$$

where the renormalization constant Z_ψ comes from ''wave-function'' renormalization (a rescaling of ψ) and, in the minimal subtraction scheme, is given by[32,33]

$$Z_\psi = 1 - \frac{1}{\epsilon}\overline{u^2} + O(\overline{u^3}). \tag{2.28}$$

The renormalized ''mass'' r is defined as

$$r \equiv G_R^{-1}(0,0), \tag{2.29}$$

which, using Eqs. (2.21), (2.26), and (2.27), is related to the bare mass r_0 by

$$r = Z_\psi[r_0 - \Sigma(0,0)]. \tag{2.30}$$

Near T_c the physical response function at zero wave number and frequency behaves as $G_R(0,0) = \xi^{2-\eta}\kappa^{-\eta}$, where η is the usual correlation function exponent and ξ is the order-parameter correlation length that diverges as

$$\xi \sim |T - T_c|^{-\nu}, \tag{2.31}$$

with the critical exponent ν. Thus, from (2.29), we have

$$r = \xi^{-2+\eta}\kappa^{\eta}. \tag{2.32}$$

Since we are neglecting magnetic fluctuations and working at the ''uncharged'' fixed point, the renormalized charge, e, is simply the bare charge: $e = e_0$. Finally, the bare relaxation rate Γ_0, appearing in the dynamic response function (2.26) is related to the renormalized relaxation rate Γ by

$$\frac{1}{\Gamma_0} = Z_\Gamma \frac{1}{\Gamma}, \tag{2.33}$$

where, from minimal subtraction, the renormalization constant Z_Γ for this relaxational model is[30,33]

$$Z_\Gamma = 1 - \frac{c}{\epsilon}\overline{u^2} + O(\overline{u^3}). \tag{2.34}$$

The constant c is given by Eq. (1.6).

Even after we renormalize the conductivity as described above, some poles in ϵ will remain. These poles are due to UV divergences in the theory for the conductivity that appear even at the Gaussian level and have nothing to do with the critical behavior. These poles must be eliminated by adding a constant to the conductivity, as will be discussed in Sec. VI.

Near T_c, as one probes the long-wavelength physics, the coupling $\overline{u}$ flows towards the fixed-point value $\overline{u}^*$ determined by the IR-stable zeros of the renormalization-group beta function $\beta(\overline{u}^*) = 0$.[32] This mechanism is responsible for universality. To leading order in the ϵ expansion, $\overline{u}^*$ is[32,33]

$$\overline{u}^* = \frac{\epsilon}{10} + O(\epsilon^2). \tag{2.35}$$

This is the Wilson-Fisher[23] fixed point for the XY model. The correlation function exponent η is related to Z_ψ, (2.28) and has the following expansion in $\overline{u}^*$:

$$\eta = 2(\overline{u}^*)^2 + O[(\overline{u}^*)^3]. \tag{2.36}$$

The result $\nu \approx 2/3$ quoted in the Introduction, which also appears in Eq. (2.31), is an extrapolation of the ϵ-expansion result to three dimensions. Finally, the dynamic exponent z is related to Z_Γ (2.34) for the relaxational dynamics, and is given by $z = 2 + c\,\eta$.

Our calculational strategy in what follows is to anticipate that $\overline{u}$ will be $O(\epsilon)$ and to keep terms up to $O(\overline{u^2})$ $[O(u^2)]$ since we will calculate to $O(\epsilon^2)$. It is advantageous to initially keep $\overline{u}$ in the calculation and expand everything else in powers of ϵ since this provides a check on whether the poles in ϵ have been minimally subtracted at each order in $\overline{u}$. Finally, by using the fixed-point value $\overline{u}^*$ for the coupling, and reorganizing the theory as an expansion in ϵ, the IR divergences near criticality can be sensibly treated and lead to corrections to the Gaussian exponents and scaling function.

III. THE CONDUCTIVITY IN THE GAUSSIAN APPROXIMATION

We now review earlier work on the ac conductivity involving noninteracting, Gaussian fluctuations,[9,10] and set $u_0 = 0$ in Eq. (2.2). In the Gaussian approximation the connected piece of the conductivity, Eq. (2.17), is zero. Thus, from Eqs. (2.15) and (2.16) one has

$$\sigma'(\omega) = \frac{2e_0^2}{d}\int_{k_1\omega_1}^{\Lambda} k_1^2 C_0(\mathbf{k}_1,\omega_1) C_0(\mathbf{k}_1,\omega_1+\omega), \tag{3.1}$$

where C_0 is given by (2.23). The calculation of the integral in Eq. (3.1) involves a contour integration over the frequency variable, and then a straightforward evaluation of the remaining wave-vector integral, with the cutoff Λ set to infinity. The complex conductivity takes the form:[9,10]

$$\sigma(\omega) = \frac{e_0^2}{2\Gamma_0}\overline{\sigma}\frac{\xi_0^{4-d}}{4-d} S_G(y_0), \tag{3.2}$$

where

$$\overline{\sigma} = \frac{S_d}{(2\pi)^d}\Gamma(d/2)\Gamma(3-d/2) \tag{3.3}$$

and the scaled frequency y_0 is

$$y_0 = \frac{\omega\xi_0^2}{2\Gamma_0}. \tag{3.4}$$

The Gaussian order-parameter correlation length ξ_0 is defined as

$$\xi_0 \equiv r_0^{-1/2}, \tag{3.5}$$

thus $\xi_0 \sim |T - T_{c0}|^{-1/2}$ and $\nu = 1/2$ in the Gaussian theory. The real part of the scaling form S_G is computed from Eq. (3.1) to be

$$S'_G(y_0) = \frac{8}{d(d-2)} \frac{1}{y_0^2}\left[1 - (1+y_0^2)^{d/4} \cos\left(\frac{d}{2}\tan^{-1} y_0\right)\right]. \tag{3.6}$$

The imaginary part of the conductivity is obtained from Eq. (3.6) using the Kramers-Kronig relations. The result for the complex scaling form is then

$$S_G(y_0) = \frac{8}{d(d-2)} \frac{1}{y_0^2}\left[1 - \frac{d}{2} i y_0 - (1 - i y_0)^{d/2}\right]. \tag{3.7}$$

The Gaussian result, Eq. (3.2) with the definition (3.4), satisfies the FFH hypothesis (1.1) with $z = 2$.

We note two properties of these results that will be important later. The first is that Eq. (3.2) has a factor of $\epsilon = 4 - d$ in the denominator. This is a consequence of setting the cutoff Λ to infinity, and indicates that even the Gaussian theory is sensitive to the cutoff in four dimensions. The second property is that S'_G (3.6) has the ϵ expansion

$$S'_G(y_0) = 1 + \sum_{i=1}^{\infty} \epsilon^i S_i(y_0). \tag{3.8}$$

The coefficient of ϵ in Eq. (3.8),

$$S_1(y_0) = \frac{3}{4} + \frac{1}{4y_0^2}[(1-y_0^2)\ln(1+y_0^2) - 4y_0 \tan^{-1} y_0], \tag{3.9}$$

is interesting because it appears later in both the disconnected and the connected pieces of the conductivity.

IV. DISCONNECTED PIECE OF THE CONDUCTIVITY

To go beyond the Gaussian theory requires the calculation of both the full two-point correlation function (2.7), including self-energy corrections, and the four-point average (2.18) which appear in the conductivity through Eqs. (2.16) and (2.17). The calculations must be performed to $O(u^2)$, where the first corrections to the Gaussian result $z = 2$ occur. In this section we examine the disconnected piece of the conductivity (2.16). The next section tackles the connected piece.

We first dimensionally regularize and renormalize the theory as outlined in Sec. II D. From Eq. (2.16), the disconnected contribution to the conductivity is then

$$\sigma^{(2)}(\omega) = \frac{2e^2}{d} \int_{k_1 \omega_1} k_1^2 C(\mathbf{k}_1, \omega_1) C(\mathbf{k}_1, \omega_1 + \omega), \tag{4.1}$$

where C is the full correlation function (2.7), including self-energy corrections. We will calculate the response function G (2.9) to $O(u^2)$ and use the fluctuation-dissipation relation (2.10) to get C. With the definition (2.30) of the renormalized mass, r, the inverse response function (2.26) may be written as

$$G^{-1}(\mathbf{k}, \omega) = G_0^{-1}(\mathbf{k}, \omega) - [\Sigma(\mathbf{k}, \omega) - \Sigma(0,0)], \tag{4.2}$$

where now

$$r_0 \to r/Z_\psi, \tag{4.3}$$

$$\Gamma_0 \to \Gamma/Z_\Gamma \tag{4.4}$$

in G_0 (2.21) and C_0 (2.23). To $O(u^2)$ only the ''Saturn'' diagram $\Sigma_s(\mathbf{k}, \omega)$ shown in Fig. 3 contributes to Eq. (4.2) since, to this order, it is the only piece of the self-energy that is wave-vector and frequency dependent. Applying the rules outlined in Sec. II C to Fig. 3 gives

$$\Sigma_s(\mathbf{k}, \omega) = 6u^2 \int_{k_2 \omega_2 k_3 \omega_3} C_0(\mathbf{k}_2, \omega_2) C_0(\mathbf{k}_3, \omega_3) \times G_0(\mathbf{k} - \mathbf{k}_2 - \mathbf{k}_3, \omega - \omega_2 - \omega_3). \tag{4.5}$$

The correlation function C is then obtained from Eq. (2.10) and (4.2):

$$C(\mathbf{k}, \omega) = C_0(\mathbf{k}, \omega) + \frac{2}{\omega} \mathrm{Im}\{G_0^2(\mathbf{k}, \omega)[\Sigma_s(\mathbf{k}, \omega) - \Sigma_s(0,0)]\} + O(u^3). \tag{4.6}$$

Thus the disconnected piece of the conductivity (4.1) can be expressed in terms of the integrals

$$I_1(\omega) = \frac{2e^2}{d} \int_{k_1 \omega_1} k_1^2 C_0(\mathbf{k}_1, \omega_1) C_0(\mathbf{k}_1, \omega_1 + \omega) \tag{4.7}$$

and

$$I_2(\omega) = \frac{4e^2}{d} \mathrm{Im} \int_{k_1 \omega_1} k_1^2 C_0(\mathbf{k}_1, \omega_1) \frac{1}{\omega_1 + \omega} G_0^2(\mathbf{k}_1, \omega_1 + \omega) \times [\Sigma_s(\mathbf{k}_1, \omega_1 + \omega) - \Sigma_s(0,0)], \tag{4.8}$$

by writing

$$\sigma^{(2)}(\omega) = I_1(\omega) + 2I_2(\omega) + O(u^3). \tag{4.9}$$

Each integral is dealt with separately below.

A. The integral I_1

The only differences between I_1 (4.7) and the starting point (3.1) of the Gaussian calculation are the substitutions: Eqs. (4.3), (4.4), and $e_0 \to e$. Transcribing the real part of the Gaussian result (3.2) gives

$$I_1(\omega) = \frac{e^2}{2\Gamma} \underline{\sigma} \kappa^{-\epsilon} \frac{x^{-\epsilon}}{\epsilon} Z_\psi^{\epsilon/2} Z_\Gamma S'_G(\tilde{y}), \tag{4.10}$$

with S'_G given in Eq. (3.6) and

$$\tilde{y} = \frac{\omega Z_\psi Z_\Gamma}{2\Gamma r}. \tag{4.11}$$

The dimensionless measure of the nearness to the transition is

$$x = \frac{\sqrt{r}}{\kappa}, \tag{4.12}$$

where the arbitrary wave-vector scale κ was introduced earlier in Eq. (2.25). From the expression (2.32) for r we have

$$x=(\xi\kappa)^{-1+\eta/2}. \tag{4.13}$$

The function $S'_G(\tilde{y})$ can be expressed in terms of the scaled frequency y,

$$y=\frac{\omega\xi^z\kappa^{z-2}}{2\Gamma} \tag{4.14}$$

with z given by Eq. (1.5), by the expansion

$$S'_G(\tilde{y})=S'_G(y)+\partial_y S'_G(y)(\tilde{y}-y)+\frac{1}{2}\partial_y^2 S'_G(y)(\tilde{y}-y)^2+\cdots, \tag{4.15}$$

where ∂_y indicates a derivative with respect to y. The results (2.28) for Z_ψ, (2.32) for r and (2.34) for Z_Γ are used to obtain the following relation between $\tilde{y}$ and y:

$$\tilde{y}-y=y(c+1)\left(\eta\ln x-\frac{1}{\epsilon}\overline{u^2}\right)+O(\overline{u^2}\epsilon). \tag{4.16}$$

Using equation (4.16), the expansion (3.8) of S'_G, and the fact that η (2.36) is $O(\epsilon^2)$, we write Eq. (4.15) as

$$\begin{aligned}S'_G(\tilde{y})=&1+\epsilon S_1(y)+\epsilon^2 S_2(y)+\epsilon^3 S_3(y)+\epsilon(c+1)\\&\times\left(\eta\ln x-\frac{1}{\epsilon}\overline{u^2}\right)[y\partial_y S_1(y)+\epsilon y\partial_y S_2(y)]\\&+O(\overline{u^2}\epsilon^2,\epsilon^4).\end{aligned} \tag{4.17}$$

We now use the expansions (2.28) of Z_ψ and (2.34) of Z_Γ together with Eq. (4.17) to write I_1 (4.10) as a series in $\overline{u}$, with coefficients expanded in powers of ϵ. Terms of $O(\overline{u^2}\epsilon,\epsilon^3)$ and higher are neglected [since the fixed-point value $\overline{u}^*$ (2.35) is $O(\epsilon)$ we are effectively working to $O(\epsilon^2)$]. The result, written in a form that will be convenient for later analysis, is

$$\begin{aligned}I_1(\omega)=&\frac{e^2}{2\Gamma}\overline{\sigma}\kappa^{-\epsilon}\left(1-\frac{1}{2}\overline{u^2}\right)\left\{-\frac{c}{\epsilon^2}\overline{u^2}+\frac{1}{\epsilon}\right.\\&+\frac{c}{\epsilon}\overline{u^2}\ln x-\frac{c}{\epsilon}\overline{u^2}S_1(y)-\frac{c+1}{\epsilon}\overline{u^2}y\partial_y S_1(y)-\ln x\\&+\frac{\epsilon-c\overline{u^2}}{2}(\ln x)^2-\frac{\epsilon^2}{6}(\ln x)^3+\left[1-(\epsilon-c\overline{u^2})\ln x\right.\\&\left.+\frac{\epsilon^2}{2}(\ln x)^2\right]S_1(y)+(\epsilon-c\overline{u^2})(1-\epsilon\ln x)S_2(y)\\&+\epsilon^2 S_3(y)+(c+1)(\eta+\overline{u^2})y\partial_y S_1(y)\ln x\\&\left.-(c+1)\overline{u^2}y\partial_y S_2(y)+O(\overline{u^2}\epsilon,\epsilon^3)\right\}.\end{aligned} \tag{4.18}$$

B. The integral I_2

The calculation of I_2, Eq. (4.8), is involved so we only outline it here. The first step is to rescale the internal wave vectors and frequencies in Eq. (4.8) by

$$\mathbf{k}_i\to\sqrt{r}\mathbf{k}'_i \tag{4.19}$$

$$\omega_i\to\Gamma r\omega'_i, \tag{4.20}$$

where $i=1,2,3$ (remember that Σ_s contains an integral over $\mathbf{k}_2\omega_2\mathbf{k}_3\omega_3$), and write

$$I_2(\omega)=\frac{12e^2}{d\Gamma}\kappa^{-\epsilon}(u\kappa^{-\epsilon})^2x^{-3\epsilon}\tilde{I}_2(y). \tag{4.21}$$

The dimensionless integral in Eq. (4.21),

$$\begin{aligned}\tilde{I}_2(y)=&16\,\mathrm{Im}\int_{k_1\omega_1k_2\omega_2k_3\omega_3}k_1^2\tilde{C}_0(\mathbf{k}_1,\omega_1)\frac{1}{\omega_1+2y}\\&\times\tilde{G}_0^2(\mathbf{k}_1,\omega_1+2y)\tilde{C}_0(\mathbf{k}_2,\omega_2)\tilde{C}_0(\mathbf{k}_3,\omega_3)\\&\times[\tilde{G}_0(\mathbf{k}_1-\mathbf{k}_2-\mathbf{k}_3,2y+\omega_1-\omega_2-\omega_3)\\&-\tilde{G}_0(-\mathbf{k}_2-\mathbf{k}_3,-\omega_2-\omega_3)],\end{aligned} \tag{4.22}$$

is written in terms of the dimensionless functions

$$\tilde{G}_0(\mathbf{k},\omega)=\frac{1}{-i\omega+1+k^2} \tag{4.23}$$

and

$$\tilde{C}_0(\mathbf{k},\omega)=\frac{1}{\omega^2+(1+k^2)^2}, \tag{4.24}$$

where, for convenience, in Eq. (4.22) we have dropped the primes on the dimensionless wave vectors and dimensionless frequencies. Since I_2 is already $O(u^2)$ we have simply replaced all bare coefficients in Eq. (4.21) by renormalized ones, and used the scaled frequency y from Eq. (4.14).

The second step is to evaluate the three frequency integrals in Eq. (4.22) by contour integration. The calculation is straightforward and yields

$$\tilde{I}_2(y)=\mathrm{Re}[\tilde{I}_2^a(y)+\tilde{I}_2^b(y)+\tilde{I}_2^c(y)], \tag{4.25}$$

with

$$\begin{aligned}\tilde{I}_2^a(y)=&\int_0^1 dv(1-v)\int_{k_1k_2k_3}k_1^2\left[\frac{2}{a_1^3}-\frac{1}{(a_1+iyv)^3}\right]\\&\times\frac{1}{a_2a_3(a_2+a_3+a_4)(a_5+2iy)},\end{aligned} \tag{4.26}$$

$$\begin{aligned}\tilde{I}_2^b(y)=&3\int_0^1 dv(1-v)\int_{k_1k_2k_3}k_1^2\frac{1}{(a_1+iyv)^4a_2a_3}\\&\times\left[\frac{1}{a_2+a_3+a_4}-\frac{1}{a_2+a_3+\overline{a_4}}\right],\end{aligned} \tag{4.27}$$

$$\tilde{I}_2^c(y) = -3iy \int_0^1 dv(1-v) \int_{k_1 k_2 k_3} k_1^2 \times \frac{1}{(a_1+iyv)^4 a_2 a_3 (a_2+a_3+a_4)(a_5+2iy)}, \tag{4.28}$$

where, for convenience, we define

$$a_i \equiv 1+k_i^2, \quad i=1,2,3, \tag{4.29}$$

$$a_4 \equiv 1+(\mathbf{k}_1+\mathbf{k}_2+\mathbf{k}_3)^2, \tag{4.30}$$

$$\overline{a}_4 \equiv 1+(\mathbf{k}_2+\mathbf{k}_3)^2, \tag{4.31}$$

$$a_5 \equiv a_1+a_2+a_3+a_4. \tag{4.32}$$

Note that we have used the Feynman formula

$$\frac{1}{c_1^{\alpha_1} c_2^{\alpha_2}} = \frac{\Gamma(\alpha_1+\alpha_2)}{\Gamma(\alpha_1)\Gamma(\alpha_2)} \int_0^1 dv (1-v)^{\alpha_1-1} v^{\alpha_2-1} \times \frac{1}{[(1-v)c_1+vc_2]^{\alpha_1+\alpha_2}} \tag{4.33}$$

with the Feynman parameter v to group and simplify terms in Eqs. (4.26)–(4.28).

The final step is to evaluate the wave-vector integrals in Eqs. (4.26)–(4.28) using (4.33) and ϵ-expand the resulting integrals over Feynman parameters to $O(\epsilon^0)$. An example of this procedure appears in Appendix A. The results for Eqs. (4.26)–(4.28) are

$$\tilde{I}_2^a(y) = A_d \left[\frac{1}{6\epsilon^2} \ln\frac{4}{3} + \frac{1}{2\epsilon} f_1(y) \ln\frac{4}{3} + \frac{0.003}{\epsilon} + \mathcal{F}_2^a(y) + O(\epsilon) \right], \tag{4.34}$$

$$\tilde{I}_2^b(y) = A_d \left[-\frac{1}{12\epsilon^2} + \frac{1}{4\epsilon} f_1(y) - \frac{0.104}{\epsilon} + \mathcal{F}_2^b(y) + O(\epsilon) \right], \tag{4.35}$$

$$\tilde{I}_2^c(y) = A_d \left[-\frac{1}{2\epsilon} f_2(y) \ln\frac{4}{3} + \mathcal{F}_2^c(y) + O(\epsilon) \right], \tag{4.36}$$

where $\mathcal{F}_2^a$, $\mathcal{F}_2^b$, and $\mathcal{F}_2^c$ are $O(\epsilon^0)$ functions of y that we do not need to determine,

$$A_d = \left(\frac{S_d}{2(2\pi)^d} \right)^3 [\Gamma(2-\epsilon/2)]^2 \Gamma(3-\epsilon/2)\Gamma(1+3\epsilon/2), \tag{4.37}$$

and

$$f_1(y) = \int_0^1 dv (1-v) \ln(1+iyv), \tag{4.38}$$

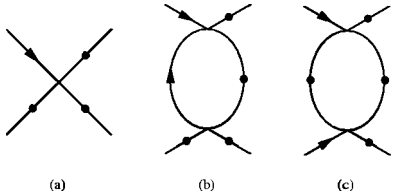

FIG. 4. The topologically distinct diagrams in the expansion of the four-point order-parameter average (2.18) to $O(u^2)$. The diagrammatic symbols are the same ones used in Fig. 3. Each diagram corresponds to several possible wave-vector and frequency assignments, which are not shown.

$$f_2(y) = iy \int_0^1 dv \frac{1-v}{1+iyv}. \tag{4.39}$$

It is straightforward to show that

$$\mathrm{Re}[f_1(y)] = -S_1(y), \tag{4.40}$$

$$\mathrm{Re}[f_2(y)] = -2S_1(y) - y\partial_y S_1(y), \tag{4.41}$$

where S_1 was given in Eq. (3.9). We use this result, along with Eqs. (4.25) and (4.34)–(4.36) to write I_2 (4.21) as a product of $\overline{u^2}$ and a series in ϵ. In particular, we have

$$2I_2(\omega) = \frac{e^2}{2\Gamma} \overline{\sigma} \kappa^{-\epsilon} \overline{u^2} \left[\frac{c-2}{3\epsilon^2} - \frac{c-2}{\epsilon} \ln x + \frac{c-2}{\epsilon} S_1(y) + \frac{(c+1)}{\epsilon} y\partial_y S_1(y) - \frac{0.787}{\epsilon} + 2.36 \ln x + \frac{3(c-2)}{2} (\ln x)^2 - 3(c-2) S_1(y) \ln x - 3(c+1) y\partial_y S_1(y) \ln x + \mathcal{D}(y) + O(\epsilon) \right], \tag{4.42}$$

with

$$\mathcal{D}(y) = 0.233 - (c-2) S_1(y) - (c+1) y\partial_y S_1(y) + 12\,\mathrm{Re}\,[\mathcal{F}_2^a(y) + \mathcal{F}_2^b(y) + \mathcal{F}_2^c(y)]. \tag{4.43}$$

V. CONNECTED PIECE OF THE CONDUCTIVITY

The topologically distinct diagrams resulting from the expansion of the connected four-point order-parameter average (2.18) to $O(u^2)$ are shown in Fig. 4. Self-energy corrections are included in these diagrams since we have renormalized the theory, following dimensional regularization. The algebraic expressions for each allowed permutation of wave vector and frequency in these diagrams is inserted in $\sigma^{(4)}$ (2.17), thereby giving a contribution to the conductivity. The $O(u)$ diagram in Fig. 4(a) does not contribute to the conductivity since in this case the integral (2.17) separates into a product of odd integrals over $\mathbf{k}_1$ and $\mathbf{k}_2$. The remaining diagrams in Fig. 4 are $O(u^2)$, and produce

$$\sigma^{(4)}(\omega) = -\frac{128e^2}{d\Gamma}\kappa^{-\epsilon}(u\kappa^{-\epsilon})^2 x^{-3\epsilon} \times \mathrm{Re}[4\tilde{I}_b(y) + \tilde{I}_c^{(1)}(y) + \tilde{I}_c^{(2)}(y)] \quad (5.1)$$

when inserted into Eq. (2.17). The diagram in Fig. 4(b) is responsible for the contribution

$$\tilde{I}_b(y) = \int_{k_1\omega_1 k_2\omega_2 k_3\omega_3} \mathbf{k}_1\cdot\mathbf{k}_2 \tilde{G}_0(\mathbf{k}_1,\omega_1)\tilde{C}_0(\mathbf{k}_1,\omega_1-2y) \times \tilde{C}_0(\mathbf{k}_2,\omega_2)\tilde{C}_0(\mathbf{k}_2,\omega_2+2y)\tilde{G}_0(\mathbf{k}_3,\omega_3) \times \tilde{C}_0(\mathbf{k}_1+\mathbf{k}_2+\mathbf{k}_3,\omega_1+\omega_2-\omega_3) \quad (5.2)$$

in Eq. (5.1) with y defined in Eq. (4.14) and $\tilde{G}_0$ and $\tilde{C}_0$ given by Eqs. (4.23) and (4.24), respectively. The diagram in Fig. 4(c) produces the other two integrals,

$$\tilde{I}_c^{(1)}(y) = \int_{k_1\omega_1 k_2\omega_2 k_3\omega_3} \mathbf{k}_1\cdot\mathbf{k}_2 \tilde{G}_0(\mathbf{k}_1,\omega_1)\tilde{G}_0(\mathbf{k}_1,2y-\omega_1) \times \tilde{C}_0(\mathbf{k}_2,\omega_2)\tilde{C}_0(\mathbf{k}_2,\omega_2+2y)\tilde{C}_0(\mathbf{k}_3,\omega_3) \times \tilde{C}_0(\mathbf{k}_1+\mathbf{k}_2+\mathbf{k}_3,\omega_1+\omega_2+\omega_3) \quad (5.3)$$

and

$$\tilde{I}_c^{(2)}(y) = \int_{k_1\omega_1 k_2\omega_2 k_3\omega_3} \mathbf{k}_1\cdot\mathbf{k}_2 \tilde{G}_0(\mathbf{k}_1,\omega_1) \times \tilde{C}_0(\mathbf{k}_1,\omega_1-2y)\tilde{C}_0(\mathbf{k}_2,\omega_2)\tilde{G}_0(\mathbf{k}_2,-2y-\omega_2) \times \tilde{C}_0(\mathbf{k}_3,\omega_3)\tilde{C}_0(\mathbf{k}_1+\mathbf{k}_2+\mathbf{k}_3,\omega_1+\omega_2+\omega_3), \quad (5.4)$$

in Eq. (5.1). As with the integral $\tilde{I}_2(y)$ (4.22) for the disconnected piece, we evaluate the frequency integrals in Eqs. (5.2)–(5.4) with contour integration and use the Feynman formula (4.33) to perform the wave-vector integrals. Upon ϵ-expanding the results we have

$$\tilde{I}_b(y) = -\frac{A_d}{96}\left[\left(\frac{1}{4}-\frac{1}{2}\ln\frac{4}{3}\right)\frac{1}{\epsilon^2} - \left(\frac{3}{4}-\frac{3}{2}\ln\frac{4}{3}\right)\frac{1}{\epsilon}\mathrm{Re}[f_1(y)] + \frac{0.057}{\epsilon} + \mathcal{F}_b(y) + O(\epsilon)\right], \quad (5.5)$$

$$\tilde{I}_c^{(1)}(y) = -\frac{A_d}{96}\left[\frac{2}{\epsilon^2}\ln\frac{4}{3} - \frac{6}{\epsilon}\ln\frac{4}{3}\mathrm{Re}[f_1(y)] + \frac{0.279}{\epsilon} + \mathcal{F}_c^{(1)}(y) + O(\epsilon)\right], \quad (5.6)$$

$$\tilde{I}_c^{(2)}(y) = -\frac{A_d}{96}\left[\frac{0.618}{\epsilon} + \mathcal{F}_c^{(2)}(y) + O(\epsilon)\right], \quad (5.7)$$

where A_d and f_1 were defined in Eqs. (4.37) and (4.38), respectively. As before, $\mathcal{F}_b$, $\mathcal{F}_c^{(1)}$, and $\mathcal{F}_c^{(2)}$ are $O(\epsilon^0)$ functions of y that do not need to be determined. Equations (5.5)–(5.7) are substituted into Eq. (5.1) and the result, expressed in terms of a product of $\overline{u^2}$ and a series in ϵ, is

$$\sigma^{(4)}(\omega) = \frac{e^2}{2\Gamma}\overline{\sigma}\kappa^{-\epsilon}\overline{u^2}\left[\frac{2}{3\epsilon^2} - \frac{2}{\epsilon}\ln x + \frac{2}{\epsilon}S_1(y) + \frac{0.086}{\epsilon} - 0.258\ln x + 3(\ln x)^2 - 6S_1(y)\ln x + \mathcal{C}(y) + O(\epsilon)\right], \quad (5.8)$$

where

$$\mathcal{C}(y) = 0.787 - 2S_1(y) + \frac{2}{3}\mathrm{Re}[4\mathcal{F}_b(y) + \mathcal{F}_c^{(1)}(y) + \mathcal{F}_c^{(2)}(y)]. \quad (5.9)$$

In Eq. (5.8) we have used the relation (4.40) between f_1 and S_1, Eq. (3.9).

VI. ADDITIVE RENORMALIZATION OF THE CONDUCTIVITY

The real part of the conductivity (2.15) is a sum of the disconnected contributions, Eqs. (4.18) and (4.42), and the connected piece, Eq. (5.8):

$$\sigma'(\omega) = \frac{e^2}{2\Gamma}\overline{\sigma}\kappa^{-\epsilon}(1-2.6\overline{u^2})\left\{\frac{1}{\epsilon} - \frac{2}{3\epsilon^2}c\overline{u^2} + \frac{1.4}{\epsilon}\overline{u^2} - \ln x + \frac{\epsilon+2c\overline{u^2}}{2}(\ln x)^2 - \frac{\epsilon^2}{6}(\ln x)^3 + \left[1-(\epsilon+2c\overline{u^2})\ln x + \frac{\epsilon^2}{2}(\ln x)^2\right]S_1(y) + (\epsilon+2c\overline{u^2})(1-\epsilon\ln x)S_2(y) + (c+1)(\eta-2\overline{u^2})y\partial_y S_1(y)\ln x + \overline{u^2}\mathcal{F}(y) + O(\overline{u^2}\epsilon,\epsilon^3)\right\}, \quad (6.1)$$

where

$$\mathcal{F}(y) = 2.1S_1(y) - 3cS_2(y) + \frac{\epsilon^2}{\overline{u^2}}S_3(y) + \mathcal{D}(y) + \mathcal{C}(y) - (c+1)y\partial_y S_2(y) \quad (6.2)$$

is an $O(\epsilon^0)$ function of y [remember that $\overline{u}$ is $O(\epsilon)$]. Even after renormalizing the bare quantities in the theory some poles in ϵ remain in Eq. (6.1). In fact, this problem arises even in the Gaussian theory [the $1/\epsilon$ term in (6.1)] and indicates that we must be more careful when we set the cutoff Λ to infinity. We should write the conductivity for $d<4$ as

$$\sigma'(\omega;d,\Lambda) = \sigma'(\omega;d,\infty) - A(\omega;d,\Lambda), \quad (6.3)$$

with

$$A(\omega;d,\Lambda) = \sigma'(\omega,d,\infty) - \sigma'(\omega;d,\Lambda). \quad (6.4)$$

The $\sigma'(\omega;d,\infty)$ term in Eq. (6.3) is just Eq. (6.1). By subtracting A (6.4) from $\sigma'(\omega;d,\infty)$ we render the conductivity finite in four dimensions, since we recover the theory with finite Λ. At low frequencies, near T_c, we expect to be able to approximate A by its value at T_c and $\omega=0$: near criticality, the IR singularities, which appear in $\sigma'(\omega;d,\infty)$, are absent in A since only UV physics contributes to the difference in (6.4). In the minimal subtraction scheme the poles of $\sigma'(\omega=0;d,\infty)$ which contain no singular temperature dependence are simply subtracted from Eq. (6.1). This situation is reminiscent of the additive renormalization of the specific heat in the static theory.[32]

Inspection of Eq. (6.1) gives

$$A=\frac{e^2}{2\Gamma}\bar{\sigma}\kappa^{-\epsilon}(1-2.6\bar{u^2})\left[\frac{1}{\epsilon}-\frac{2}{3\epsilon^2}c\bar{u^2}+\frac{1.4}{\epsilon}\bar{u^2}+O(\bar{u^3})\right], \tag{6.5}$$

and thus we write the fully renormalized conductivity $\sigma'_R(\omega)=\sigma'(\omega)-A$ as

$$\begin{aligned}\sigma'_R(\omega)=\frac{e^2}{2\Gamma}\bar{\sigma}\kappa^{-\epsilon}(1-2.6\bar{u^2})\Bigg\{&-\ln x+\frac{\epsilon+2c\bar{u^2}}{2}(\ln x)^2\\&-\frac{\epsilon^2}{6}(\ln x)^3+\Bigg[1-(\epsilon+2c\bar{u^2})\ln x\\&+\frac{\epsilon^2}{2}(\ln x)^2\Bigg]S_1(y)+(\epsilon+2c\bar{u^2})(1-\epsilon\ln x)S_2(y)\\&+(c+1)(\eta-2\bar{u^2})y\partial_y S_1(y)\ln x+\bar{u^2}\mathcal{F}(y)\\&+O(\bar{u^2}\epsilon,\epsilon^3)\Bigg\}.\end{aligned} \tag{6.6}$$

Now we have a theory that is UV convergent as $\epsilon\to 0$, but has IR divergences as $T\to T_c$ and $x\to 0$. Near four dimensions, the coupling constant $\bar{u}$ flows in the IR to its XY-model fixed-point value $\bar{u}^*$ [see Eq. (2.35)], with $\eta=2(\bar{u}^*)^2$ [see Eq. (2.36)] and, after resumming, the series in ϵ takes the form

$$\sigma'_R(\omega)=\frac{e^2}{2\Gamma}\bar{\sigma}\kappa^{-\epsilon}\left[\frac{x^{-p}-1}{p}+x^{-p}S_1(y)+px^{-p}S_2(y)+\frac{p^2}{100}\mathcal{F}(y)+O(p^3)\right], \tag{6.7}$$

where p is $O(\epsilon)$ and is defined as

$$p=\epsilon+c\eta \tag{6.8}$$

$$=2-d+z+O(\epsilon^3) \tag{6.9}$$

$$=\frac{2}{z}(2-d+z)+O(\epsilon^3). \tag{6.10}$$

The $(1-2.6\bar{u^2})$ factor in Eq. (6.7) has been absorbed by changing the normalization of $\sigma'_R(\omega=0)$. As $T\to T_c$ and $x\to 0$ terms proportional x^{-p} in Eq. (6.7) dominate the conductivity.[34] From Eq. (4.13) we have

$$x^{-p}=(\xi\kappa)^p[1+O(\epsilon^3)], \tag{6.11}$$

and as $T\to T_c$ we write

$$\sigma'_R(\omega)=\frac{e^2}{2\Gamma}\bar{\sigma}\kappa^{-\epsilon}\frac{(\xi\kappa)^p}{p}[1+pS_1(y)+p^2S_2(y)+O(p^3)]. \tag{6.12}$$

In Eq. (6.12), the series in p coincides, to $O(p^2)$, with the ϵ expansion for the Gaussian scaling form S'_G, Eq. (3.8). Thus, by resumming the series in Eq. (6.12) we obtain, correct to $O(\epsilon^2)$, the Gaussian scaling form S'_G, Eq. (3.6), now as a function of the critical scaled frequency y (4.14) and with occurrences of ϵ replaced by p. Resummation of the series in Eq. (6.12) is necessary if one is to have a scaling function which is uniform in y (here uniform means the expansion is asymptotic in ϵ for all y). In particular, resummation is necessary if one is to recover the power-law behavior (1.2) at large-scaled frequencies.

The final result for complex ac conductivity in the critical regime is then (dropping the R suffix)

$$\sigma(\omega)=\frac{e^2}{2\Gamma}\bar{\sigma}\kappa^{-\epsilon}\frac{(\xi\kappa)^{2-d+z}}{(2-d+z)}[S(y)+O(\epsilon^3)], \tag{6.13}$$

with the scaled frequency y given by Eq. (4.14) and the universal complex scaling function $S(y)$ given by Eq. (1.7).

VII. COMPARISON WITH EXPERIMENT

It is instructive to compare the universal function $S(y)$, Eq. (1.7), for the critical theory (extrapolated to $d=3$), with both the prediction of the Gaussian theory, Eq. (3.7), and the experimental results of Ref. 18. Strictly speaking, it is inconsistent to compare scaled data from different theories and experiments if the axes have been scaled using different exponents. However, for the sake of comparison, we take the viewpoint that the theory and experiment each determine a particular universal functional dependence $S(y)$ and ignore exactly how $S(y)$ and y are achieved.

In this spirit, the magnitude of $S(y)$ as a function of y is plotted on a log-log scale in Fig. 1 for the critical and Gaussian theories. Since $z\gtrsim 2$ in the critical theory, the power-law behavior at large y [a consequence of (1.2)] for the critical theory lies only slightly below the Gaussian theory.

In Fig. 5, the critical theory is compared with measurements of the microwave conductivity of a thin-film sample of $YBa_2Cu_3O_{7-\delta}$ in the range 45 MHz–45 GHz near T_c.[18] In this experiment, the exponent $z=2.65\pm 0.3$ and the transition temperature $T_c=89.1\pm 0.1$ K, were determined from the power-law behavior (1.2) expected at T_c. The best scaling collapse of the data determined the value $\nu=1.0\pm 0.2$ for the static exponent.[35] In Fig. 5(a) the magnitude of $S(y)$ is again plotted as a function of y on a log-log scale. The Gaussian theory is not plotted since it lies so close to the critical theory. Since Γ, κ, and the prefactor of ξ, which appear in both the scaled frequency y (4.14) and the prefactor to the conductivity (6.13), are parameters in the TDGL theory, there is freedom to choose the horizontal and vertical positioning of the theory so as to give the best fit to the data. As with the Gaussian theory, the critical theory fits the experimental scaling curve well over almost four decades in scaled

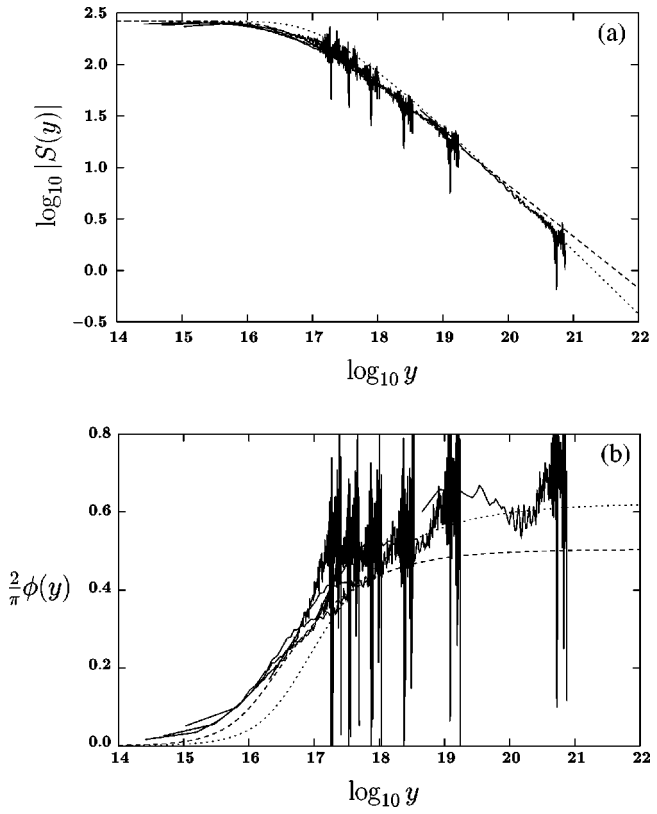

FIG. 5. Comparison between the scaled ac conductivity data from Booth *et al.*, Ref. 18, on YBCO and the relaxational 3D *XY* critical theory. (a) The scaling function $S(y)$, Eq. (1.7), using the relaxational 3D *XY* value $z=2.015$ (dashed curve) and using the experimental value $z=2.65$ (dotted curve) are compared with the experimental results (solid curves). The magnitude of $S(y)$ is plotted against y on a log-log scale. The theory is fit to the experiment using horizontal and vertical offsets (the horizontal offset depends on the value of z used). (b) The normalized phase, $2\phi(y)/\pi$, of the conductivity is plotted against $\log_{10}y$ for the relaxational 3D *XY* critical theory with $z=2.015$ (dashed curve), the theory using the experimental value $z=2.65$ (dotted curve) and experiment (solid curves). The horizontal offsets are the same as in (a).

frequency y, but deviates from the experimental data taken nearest to T_c.

The dynamic exponent for the relaxational 3D *XY* model is known to have the value $z\approx 2.015$. Nevertheless, it is instructive to consider the z appearing in $S(y)$, Eq. (1.7), as an adjustable parameter. By choosing the experimental value $z=2.65$ and adjusting the horizontal offset of the theory in Fig. 5, a better fit to the experimental data closest to T_c is achieved—at the expense of worse agreement with the rest of the data. This comparison emphasizes that the experimental value $z=2.65$ seems to originate in the data set taken closest to T_c.

The phase $\phi(y)$, Eq. (1.3), of the conductivity is plotted against $\log_{10}y$ in Fig. 5(b) for the critical theory ($z=2.015$), ''pseudo''-theory ($z=2.65$) and the experiment.[18] As with the Gaussian theory, the critical theory predicts a smaller phase near T_c than seen experimentally. The ''pseudo'' theory is in better agreement with experiment near T_c than the critical theory, but again does a poorer job fitting the rest of the curve.

VIII. CONCLUSIONS

We have examined a theory for the ac conductivity of a superconductor that includes the strong, interacting order-parameter fluctuations expected near criticality. The FFH scaling hypothesis, Eq. (1.1), is shown to hold at $O(\epsilon^2)$ in the ϵ expansion for relaxational *XY*-model critical dynamics. The universal scaling function $S(y)$ appearing in Eq. (1.1) is explicitly calculated to $O(\epsilon^2)$ for this dynamics, with the result given in Eq. (1.7). The frequency and phase behavior expected at T_c, Eqs. (1.2) and (1.4), respectively, is demonstrated. The critical scaling function $S(y)$ generalizes the Gaussian result, Eq. (3.7), and reduces to it when $z=2$. These results are quite general and hold, in the critical regime, for any bulk superconductor described by a complex order parameter with relaxational dynamics.

Since $z\approx 2$ for this model, the scaling function of Eq. (1.7) is, for practical purposes, indistinguishable from the prediction of the Gaussian theory (see Fig. 1). Therefore, in a measurement of the ac conductivity, the only indication of a crossover from the Gaussian to critical fluctuation regime would be a crossover in the static exponent ν. This may explain why the Gaussian theory fits the experimental data of Booth *et al.*[18] so well over much of the curve in Fig. 5, even though the experiment is supposedly accessing the critical regime.

The inclusion of critical order-parameter fluctuations in the framework of relaxational dynamics does not seem sufficient to explain the deviation between the Gaussian scaling form and experiment[18] observed near T_c (see Fig. 5). As highlighted by the fit of the ''pseudo'' theory in Fig. 5, this deviation is connected to the large value $z=2.65$ obtained in the experiment, which cannot be explained within any present theory.[36] It is possible that this discrepancy may be due to the strong influence that uncertainties in the experimental determination of T_c have on the scaling of the data closest to T_c. More ac conductivity measurements with higher temperature resolution near T_c may resolve this issue, allow a more accurate determination of z, and provide a check on the scaling collapse for large y. It is also possible that the films studied contain strong disorder, which could affect the scaling near T_c.

In this paper we have identified and dealt with the technical challenges involved in the organization and renormalization of the theory for the ac conductivity in the critical region. This work serves as a basis for examining more complicated models, such as model F of Hohenberg and Halperin[21] involving reversible couplings to a conserved energy-mass density field, as in superfluid ^{4}He. In three dimensions $z=3/2$ for model F,[30,37] which, although not observed in the ac conductivity data,[18] is seen in some dc conductivity experiments[4,12,14] and simulations.[38] Another extension of the present theory is to consider a nonzero magnetic field, with the aim of examining the crossover from the zero-field critical scaling of the 3D *XY* model to the lowest-Landau-level scaling which obtains in high fields.[13,39]

ACKNOWLEDGMENTS

The authors would like to thank Gene Mazenko and Andrei Varlamov for useful comments, and Steve Anlage for

providing his experimental data. This work was supported by NSERC of Canada and NSF Grants No. DMR 9628926 and No. PHY 9722133.

APPENDIX A

To illustrate the calculation of wave-vector integrals, we use this appendix to provide the details of the ϵ expansion of $\tilde{I}_2^a(y)$, Eq. (4.26), which is reproduced, in the notation of Sec. IV B, as

$$\tilde{I}_2^a(y)=\int_0^1 dv(1-v)\int_{k_1k_2k_3} k_1^2\left[\frac{2}{a_1^3}-\frac{1}{(a_1+iyv)^3}\right]\times\frac{1}{a_2a_3(a_2+a_3+a_4)(a_5+2iy)}. \tag{A1}$$

We parametrize the wave-vector factors in the denominator of Eq. (A1) in pairs using the Feynman parameterization (4.33), beginning with factors on the right containing $\mathbf{k}_3$. The denominator of the $\mathbf{k}_3$ integral is thereby transformed into a quadratic form in $\mathbf{k}_3$ and the integral is solved. The process is repeated for the remaining two wave-vector integrals, producing

$$\tilde{I}_2^a(y)=\frac{A_d}{3\epsilon}\int_0^1 dv(1-v)[2J(v=0,y)-J(v,y)] \tag{A2}$$

with

$$J(v,y)=\int_0^1 du_1du_2du_3du_4u_2(1+u_2)^{\epsilon-1}u_3^{\epsilon/2}\times(1-u_4)^2u_4^{\epsilon-1}\frac{\tilde{g}_0^{-3\epsilon/2}}{g_2^{2-\epsilon/2}\tilde{g}_1^{3-\epsilon/2}}, \tag{A3}$$

where we have defined

$$\tilde{g}_0=(1-u_4)(1+iyv)+u_4g_0, \tag{A4}$$

$$\tilde{g}_1=1+u_4(g_1-1), \tag{A5}$$

$$g_0=1-u_3+u_3(1+u_2)\{1+u_2[2+u_1(1+2iy)]\}, \tag{A6}$$

$$g_1=\frac{u_2u_3}{g_2}\{g_2[1+u_1(1+u_2)]-u_2u_3\}, \tag{A7}$$

$$g_2=1-u_3+u_2u_3(2+u_2). \tag{A8}$$

In the ϵ expansion J in Eq. (A3) is $O(\epsilon^{-1})$ at leading order. The singularity in ϵ is isolated by writing J as

$$J(v,y)=J_a(v,y)+J_b(v,y), \tag{A9}$$

where

$$J_a(v,y)=(1+iyv)^{-3\epsilon/2}\int_0^1 du_2du_3du_4u_2\times(1+u_2)^{\epsilon-1}\frac{u_3^{\epsilon/2}}{g_2^{2-\epsilon/2}}u_4^{\epsilon-1}, \tag{A10}$$

$$J_b(v,y)=\int_0^1 du_1du_2du_3du_4u_2(1+u_2)^{\epsilon-1}\frac{u_3^{\epsilon/2}}{g_2^{2-\epsilon/2}}u_4^{\epsilon-1}\times\left[(1-u_4)^2\frac{\tilde{g}_0^{-3\epsilon/2}}{\tilde{g}_1^{3-\epsilon/2}}-(1+iyv)^{-3\epsilon/2}\right]. \tag{A11}$$

In the ϵ expansion, Eq. (A10) becomes

$$J_a(v,y)=\frac{1}{\epsilon}\int_0^1 du_2du_3\frac{u_2}{g_2^2(1+u_2)}-\frac{3}{2}\times\ln(1+iyv)\int_0^1 du_2du_3\frac{u_2}{g_2^2(1+u_2)}+\int_0^1 du_2du_3\frac{u_2}{g_2^2(1+u_2)}\left[\ln(1+u_2)+\frac{1}{2}\ln u_3+\frac{1}{2}\ln g_2\right]+\epsilon\mathcal{F}_a(v,y)+O(\epsilon^2), \tag{A12}$$

where $\mathcal{F}_a(v,y)$ is a function of v and y. The integrals in Eq. (A12) are evaluated to produce

$$J_a(v,y)=\frac{1}{\epsilon}\ln\frac{4}{3}-\frac{3}{2}\ln\frac{4}{3}\times\ln(1+iyv)-0.087+\epsilon\mathcal{F}_a(v,y)+O(\epsilon^2). \tag{A13}$$

The nonsingular integral J_b, Eq. (A11), has the expansion

$$J_b(v,y)=\int_0^1 du_1du_2du_3du_4\frac{u_2}{g_2^2(1+u_2)}\frac{1}{u_4}\left[\frac{(1-u_4)^2}{\tilde{g}_1^3}-1\right]+\epsilon\mathcal{F}_b(v,y)+O(\epsilon^2)=0.103+\epsilon\mathcal{F}_b(v,y)+O(\epsilon^2), \tag{A14}$$

where $\mathcal{F}_b(v,y)$ is a function of v and y. By combining Eqs. (A13) and (A14) in Eq. (A9) we may use this result for J in $\tilde{I}_2^a$, Eq. (A2), to obtain the result quoted in Eq. (4.34), with

$$\mathcal{F}_2^a(y)=\frac{1}{3}\int_0^1 dv(1-v)\{2[\mathcal{F}_a(0,y)+\mathcal{F}_b(0,y)]-[\mathcal{F}_a(v,y)+\mathcal{F}_b(v,y)]\}. \tag{A15}$$

*Present address: Department of Physics and Astronomy, McMaster University, Hamilton, Ontario, Canada L8S 4M1. Electronic address: wickham@physics.mcmaster.ca

†Electronic address: dorsey@phys.ufl.edu

[1] S. Kamal, D.A. Bonn, N. Goldenfeld, P.J. Hirschfeld, R. Liang, and W.N. Hardy, Phys. Rev. Lett. **73**, 1845 (1994).

[2] S.M. Anlage, J. Mao, J.C. Booth, D.H. Wu, and J.L. Peng, Phys. Rev. B **53**, 2792 (1996).

[3] M.B. Salamon, J. Shi, N. Overend, and M.A. Howson, Phys. Rev. B **47**, 5520 (1993); M.B. Salamon, W. Lee, K. Ghiron, J. Shi, N. Overend, and M.A. Howson, Physica A **200**, 365 (1993).

[4] A. Pomar, A. Dìaz, M.V. Ramallo, C. Torrón, J.A. Veira, and

Félix Vidal, Physica C **218**, 257 (1993).
[5] R. Liang, D.A. Bonn, and W.N. Hardy, Phys. Rev. Lett. **76**, 835 (1996).
[6] N. Overend, M.A. Howson, and I.D. Lawrie, Phys. Rev. Lett. **72**, 3238 (1994).
[7] V. Pasler, P. Schweiss, C. Meingast, B. Obst, H. Wühl, A.I. Rykov, and S. Tajima, Phys. Rev. Lett. **81**, 1094 (1998).
[8] L.G. Aslamazov, and A.I. Larkin, Phys. Lett. **26A**, 238 (1968).
[9] H. Schmidt, Z. Phys. **216**, 336 (1968); **232**, 443 (1970).
[10] A.T. Dorsey, Phys. Rev. B **43**, 7575 (1991).
[11] M.A. Howson, N. Overend, I.D. Lawrie, and M.B. Salamon, Phys. Rev. B **51**, 11 984 (1995).
[12] W. Holm, Yu. Eltsev, and Ö. Rapp, Phys. Rev. B **51**, 11 992 (1995).
[13] K. Moloni, M. Friesen, S. Li, V. Souw, P. Metcalf, L. Hou, and M. McElfresh, Phys. Rev. Lett. **78**, 3173 (1997).
[14] J.-T. Kim, N. Goldenfeld, J. Giapintzakis, and D.M. Ginsberg, Phys. Rev. B **56**, 118 (1997).
[15] C. Dekker, R.H. Koch, B. Oh, and A. Gupta, Physica C **185-189**, 1799 (1991).
[16] J.M. Roberts, B. Brown, J. Tate, X.X. Xi, and S.N. Mao, Phys. Rev. B **51**, 15 281 (1995).
[17] K. Moloni, M. Friesen, S. Li, V. Souw, P. Metcalf, and M. McElfresh, Phys. Rev. B **56**, 14 784 (1997).
[18] J.C. Booth, D.H. Wu, S.B. Qadri, E.F. Skelton, M.S. Osofsky, A. Piqué, and S.M. Anlage, Phys. Rev. Lett. **77**, 4438 (1996).
[19] D.S. Fisher, M.P.A. Fisher, and D.A. Huse, Phys. Rev. B **43**, 130 (1991).
[20] S.-K. Ma, *Modern Theory of Critical Phenomena* (Addison-Wesley, New York, 1976).
[21] P.C. Hohenberg and B.I. Halperin, Rev. Mod. Phys. **49**, 435 (1977).
[22] Another dynamical model proposed to describe the superconducting transition is model *F* in the Hohenberg and Halperin classification (Ref. 21), where the order parameter is coupled to a reversible, conserved energy-mass density field, as in a superfluid. However, the second-sound mode produced by this coupling is expected to be gapped in the presence of the Coulomb interaction, suggesting that the critical dynamics of the superconductor may be appropriately described using the purely relaxational model *A* (Ref. 19).
[23] K.G. Wilson and M.E. Fisher, Phys. Rev. Lett. **28**, 240 (1972); K.G. Wilson, *ibid.* **28**, 548 (1972).
[24] B.I. Halperin, P.C. Hohenberg, and S.-K. Ma, Phys. Rev. Lett. **29**, 1548 (1972).
[25] B.I. Halperin, T.C. Lubensky, and S.-K. Ma, Phys. Rev. Lett. **32**, 292 (1974) first considered the possibility that, very near T_c, vector-potential fluctuations may cause the superconducting transition to be weakly first order. Subsequent calculations and simulations suggest that in type-II superconductors the transition remains second order, being either in the static universality class of the inverted 3D *XY* model [see C. Dasgupta and B.I. Halperin, Phys. Rev. Lett. **47**, 1556 (1981); P. Olsson, and S. Teitel, *ibid.* **80**, 1964 (1998)] or in a completely new static universality class [see, for example, L. Radzihovsky, Europhys. Lett. **29**, 227 (1995)]. However, even in high-T_c materials the temperature range over which vector-potential fluctuations are expected to be important is estimated to be so narrow as to be beyond present experimental resolution (Ref. 19). Thus, for present purposes, ignoring these fluctuations is justified.
[26] Microscopic mechanisms such as the Maki-Thompson terms are not considered in the TDGL model. However, these terms are expected to be less singular than the divergences considered here. For a review, see A.A. Varlamov, G. Balestrino, E. Milani, and D.V. Livanov, Adv. Phys. **48**, 655 (1999).
[27] D. Forster, *Hydrodynamic Fluctuations, Broken Symmetry, and Correlation Functions* (Addison-Wesley, New York, 1975).
[28] R. Kubo, M. Toda, and N. Hashitsume, *Statistical Physics II: Nonequilibrium Statistical Mechanics* (Springer-Verlag, New York, 1985).
[29] P.C. Martin, E.D. Siggia, and H.A. Rose, Phys. Rev. A **8**, 423 (1973).
[30] C. De Dominicis and L. Peliti, Phys. Rev. B **18**, 353 (1978).
[31] G.F. Mazenko, in *Correlation Functions and Quasiparticle Interactions in Condensed Matter*, Vol. 35 of *NATO Advanced Study Institute, Series B: Physics*, edited by J. Woods Halley (Plenum, New York, 1978).
[32] D. Amit, *Field Theory, the Renormalization Group, and Critical Phenomena* (World Scientific, Singapore, 1984).
[33] Our expressions for the renormalization constants differ slightly from those in Refs. 30 and 32 since the coupling $\bar{u}$ defined in Eq. (2.25) involves different numerical factors than the definition in Refs. 30 and 32.
[34] In Eq. (6.7) it is possible that terms of the form $p^2 x^{-p} \mathcal{F}(y)/100$ also contribute to the conductivity near T_c. To check this would, however, require a calculation correct to $O(p^3)$.
[35] If the experimental data are force fit to the 3D *XY* model exponents $\nu \approx 2/3$ and $z \approx 2.015$ using experimentally reasonable choices for T_c, the scaling collapse is much poorer than that obtained in Ref. 18.
[36] It is interesting to note that Monte Carlo simulations of vortex-loop dynamics by J. Lidmar, M. Wallin, C. Wengel, S.M. Girvin, and A.P. Young, Phys. Rev. B **58**, 2827 (1998) give $z = 2.7$ when vector-potential fluctuations are included. At present, the theory for the critical *dynamics* of the superconducting transition including vector-potential fluctuations is *terra incognita* [see, however, C.-Y. Mou, Phys. Rev. B **55**, R3378 (1997)]. It seems unlikely, though, that the experiment of Ref. 18 is accessing the regime of vector-potential fluctuations (see the discussion in Ref. 25).
[37] B.I. Halperin, P.C. Hohenberg, and E.D. Siggia, Phys. Rev. B **13**, 1299 (1976).
[38] Monte Carlo simulations of vortex-loop dynamics by H. Weber and H.J. Jensen, Phys. Rev. Lett. **78**, 2620 (1997), and Lidmar *et al.* in Ref. 36, find $z = 1.5$ for the uncharged superconducting transition. It is not clear, however, whether a connection exists between Monte Carlo vortex-loop dynamics and model *F* dynamics.
[39] S. Ullah and A.T. Dorsey, Phys. Rev. B **44**, 262 (1991); I.D. Lawrie, Phys. Rev. Lett. **79**, 131 (1997).